Publication Year	2020
Acceptance in OA	2021-11-16T15:47:19Z
Title	The accretion history of high-mass stars: An ArTéMiS pilot study of Infrared Dark Clouds
Authors	Peretto, N., Rigby, A., André, Ph., Könyves, V., Fuller, G., Zavagno, A., Schuller, F., Arzoumanian, D., Bontemps, S., Csengeri, T., Didelon,P., Duarte-Cabral, A., Palmeirim, P., PEZZUTO, Stefano, Revéret, V., Roussel, H., Shimajiri, Y.
Publisher's version (DOI)	10.1093/mnras/staa1656
Handle	http://hdl.handle.net/20.500.12386/31092
Journal	MONTHLY NOTICES OF THE ROYAL ASTRONOMICAL SOCIETY
Volume	496

sources are less fragmented than protostellar ones, and if anything, these studies show the opposite. We already know that for eight of the most massive sources from our sample, ALMA observations at ∼8000 AU resolution reveal that most of the ALMA flux comes from the brightest core (Csengeri et al. 2017), and for the one source observed at ∼500 AU resolution, a single core is identified (Csengeri et al. 2018). It is therefore likely that our conclusions remain valid even on small scales (see also Appendix E).

Another argument that seems to favour the clump-fed scenario is the shape of the upper envelope of the data point distribution in Fig. 5. As it can be seen in Fig. 8, this envelope is naturally reproduced by clump-fed tracks. Ideally, we would like to generate modelled density plots of such diagrams and compare to their observed equivalent. However, the number of sources at our disposition is currently too small to perform such an analysis. Larger number statistics would also allow us to set stronger constraints on the existence of starless sources with masses above 30 $M_\odot$ and their statistical lifetimes. By mapping all observable massive star-forming regions within a 3-kpc distance radius from the Sun, the CAFFEINE large programme on APEX with ArTéMiS aims at providing enough source statistics to build temperature versus mass density plots, allowing us to definitely conclude on the dominant scenario regulating the formation of massive stars and on the existence of a transition regime between core-fed and clump-fed star formation.

ACKNOWLEDGEMENTS

We would like to thank the referee for the report that contributed to improve the quality of this paper. N. P. acknowledges the support of the Science and Technology Facilities Council consolidated grant number ST/N000706/1. D. A. and P. P. acknowledge support from Fundação para a Ciênca e a Tecnologia (FCT) through the research grants UIDB/04434/2020 and UIDP/04434/2020. P. P. receives support from fellowship SFRH/BPD/110176/2015 funded by FCT (Portugal) and POPH/FSE (EC). A. D. C. acknowledges the support from the Royal Society University Research Fellowship (URF/R1/191609). S. B. acknowledges support by the Agence Nationale de la Recherche (France) through the project 'GENESIS' (ANR-16-CE92-0035-01). Part of this work was also supported by the European Research Council under the European Union's Seventh Framework Programme (ERC Advanced Grant Agreement No. 291294 – 'ORISTARS'). We also acknowledge the financial support of the French national programs on stellar and interstellar medium physics (PNPS and PCMI). This work is based on observations with the Atacama Pathfinder EXperiment (APEX) telescope. APEX is a collaboration between the Max Planck Institute for Radio Astronomy, the European Southern Observatory, and the Onsala Space Observatory. Swedish observations on APEX are supported through Swedish Research Council grant no. 2017-00648.

REFERENCES

Aguirre J. E. et al., 2011, ApJS, 192, 4
Andre P., Ward-Thompson D., Barsony M., 2000, in Mannings V., Boss A. P., Russell S. S., eds, Protostars and Planets IV. The University of Arizona Press, Tucson, AZ, p. 59
André P. et al., 2008, A&A, 490, L27
André P. et al., 2010, A&A, 518, L102 +
André P., Di Francesco J., Ward-Thompson D., Inutsuka S. I., Pudritz R. E., Pineda J. E., 2014, in Beuther H., Klessen R. S., Dullemond C. P., Henning T., eds, Protostars and Planets VI. The University of Arizona Press, Tucson, AZ,p. 27
André P. et al., 2016, A&A, 592, A54
André P., Arzoumanian D., Könyves V., Shimajiri Y., Palmeirim P., 2019, A&A, 629, L4
Arzoumanian D. et al., 2011, A&A, 529, L6 +
Arzoumanian D. et al., 2019, A&A, 621, A42
Barnes P. J., Muller E., Indermuehle B., O'Dougherty S. N., Lowe V., Cunningham M., Hernandez A. K., Fuller G. A., 2015, ApJ, 812, 6
Beuther H. et al., 2013, A&A, 553, A115
Beuther H. et al., 2018, A&A, 617, A100
Bonnell I. A., Vine S. G., Bate M. R., 2004, MNRAS, 349, 735
Bonnor W. B., 1956, MNRAS, 116, 351
Bontemps S., Andre P., Terebey S., Cabrit S., 1996, A&A, 311, 858
Bontemps S., Motte F., Csengeri T., Schneider N., 2010, A&A, 524, A18
Csengeri T. et al., 2014, A&A, 565, A75
Csengeri T. et al., 2017, A&A, 600, L10
Csengeri T. et al., 2018, A&A, 617, A89
Duarte-Cabral A., Bontemps S., Motte F., Hennemann M., Schneider N., André P., 2013, A&A, 558, A125
Dunham M. M., Crapsi A., Evans N. J., II, Bourke T. L., Huard T. L., Myers P. C., Kauffmann J., 2008, ApJS, 179, 249
Ebert R., 1955, ZAp, 37, 217
Elia D. et al., 2017, MNRAS, 471, 100
Ellsworth-Bowers T. P. et al., 2013, ApJ, 770, 39
Foster J. B. et al., 2013, PASA, 30, e038
Giannetti A., Wyrowski F., Leurini S., Urquhart J., Csengeri T., Menten K. M., Bronfman L., van der Tak F. F. S., 2015, A&A, 580, L7
Hildebrand R. H., 1983, QJRAS, 24, 267
Hosokawa T., Omukai K., 2009, ApJ, 691, 823
Inutsuka S.-i., Miyama S. M., 1997, ApJ, 480, 681
Könyves V. et al., 2015, A&A, 584, A91
Könyves V. et al., 2020, A&A, 635, A34
Ladjelate B. et al., 2020, A&A, 638, 74
Lee Y.-N., Hennebelle P., Chabrier G., 2017, ApJ, 847, 114
Louvet F. et al., 2019, A&A, 622, A99
McKee C. F., Offner S. S. R., 2010, ApJ, 716, 167
Men'shchikov A. et al., 2010, A&A, 518, L103
Molinari S., Pezzuto S., Cesaroni R., Brand J., Faustini F., Testi L., 2008, A&A, 481, 345
Molinari S. et al., 2010, A&A, 518, L100
Molinari S. et al., 2016, A&A, 591, A149
Moore T. J. T. et al., 2015, MNRAS, 453, 4264
Motte F., Andre P., Neri R., 1998, A&A, 336, 150
Motte F., Bontemps S., Schilke P. N., Menten K. M., Broguière D., 2007, A&A, 476, 1243
Motte F. et al., 2018a, Nature Astron., 2, 478
Motte F., Bontemps S., Louvet F., 2018b, ARA&A, 56, 41
Myers P. C., 2009, ApJ, 700, 1609
Myers P. C., 2012, ApJ, 752, 9
Offner S. S. R., McKee C. F., 2011, ApJ, 736, 53
Palau A. et al., 2013, ApJ, 762, 120
Peretto N., Fuller G. A., 2009, A&A, 505, 405
Peretto N., André P., Belloche A., 2006, A&A, 445, 979
Peretto N. et al., 2013, A&A, 555, A112
Peretto N., Lenfestey C., Fuller G. A., Traficante A., Molinari S., Thompson M. A., Ward-Thompson D., 2016, A&A, 590, A72
Ragan S. E., Heitsch F., Bergin E. A., Wilner D., 2012, ApJ, 746, 174
Reid M. J. et al., 2009, ApJ, 700, 137
Reid M. J. et al., 2014, ApJ, 783, 130
Revéret V. et al., 2014, Proceedings of the SPIE conference, 9153, 11
Rosolowsky E. W., Pineda J. E., Kauffmann J., Goodman A. A., 2008, ApJ, 679, 1338
Sanhueza P. et al., 2019, ApJ, 886, 102
Schneider N., Csengeri T., Bontemps S., Motte F., Simon R., Hennebelle P., Federrath C., Klessen R., 2010, A&A, 520, A49
Schuller F. et al., 2009, A&A, 504, 415
Smith R. J., Longmore S., Bonnell I., 2009, MNRAS, 400, 1775
Svoboda B. E. et al., 2019, ApJ, 886, 36
Terebey S., Chandler C. J., Andre P., 1993, ApJ, 414, 759

Urquhart J. S. et al., 2014, MNRAS, 443, 1555
Vázquez-Semadeni E., Palau A., Ballesteros-Paredes J., Gómez G. C., Zamora-Avilés M., 2019, MNRAS, 490, 3061
Wang P., Li Z.-Y., Abel T., Nakamura F., 2010, ApJ, 709, 27

SUPPORTING INFORMATION

Supplementary data are available at *MNRAS* online.

Table 2. Properties of the first 10 ArTéMiS sources identified in the SDC326 field.

APPENDIX A: ARTÉMIS IMAGES

In this Appendix, we present the ArTéMiS images for the SDC328, SDC340, SDC343, and SDC345 fields.

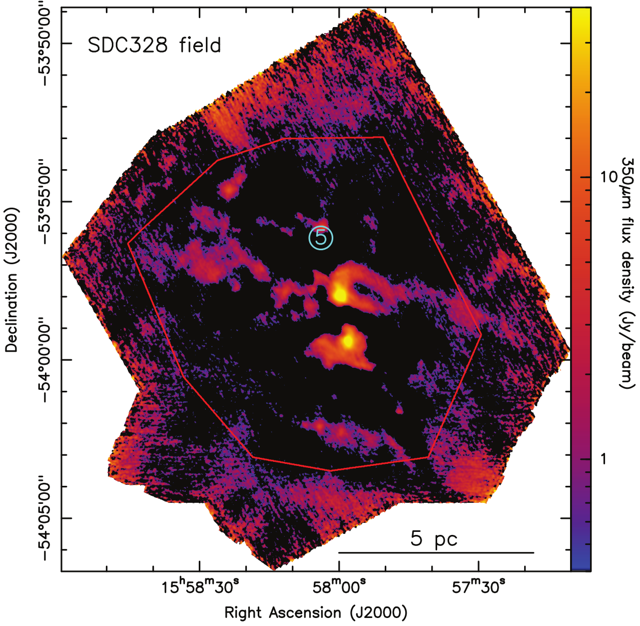

Figure A1. Same as Fig. 1 for the SDC328 field.

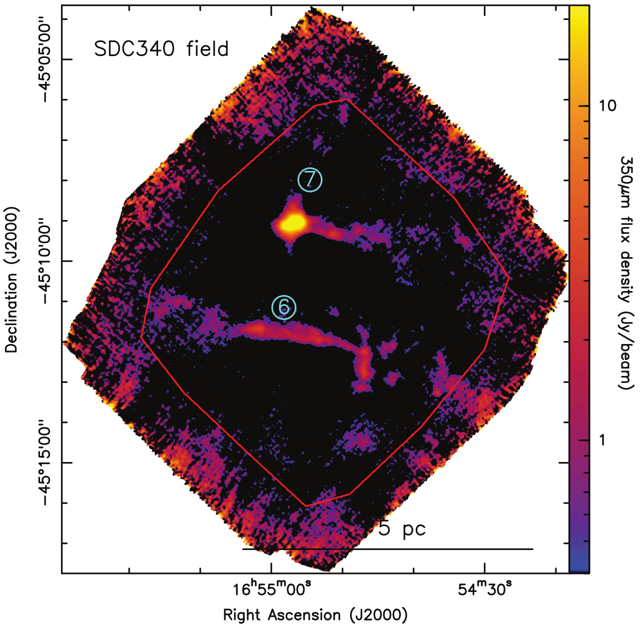

Figure A2. Same as Fig. 1 for the SDC340 field.

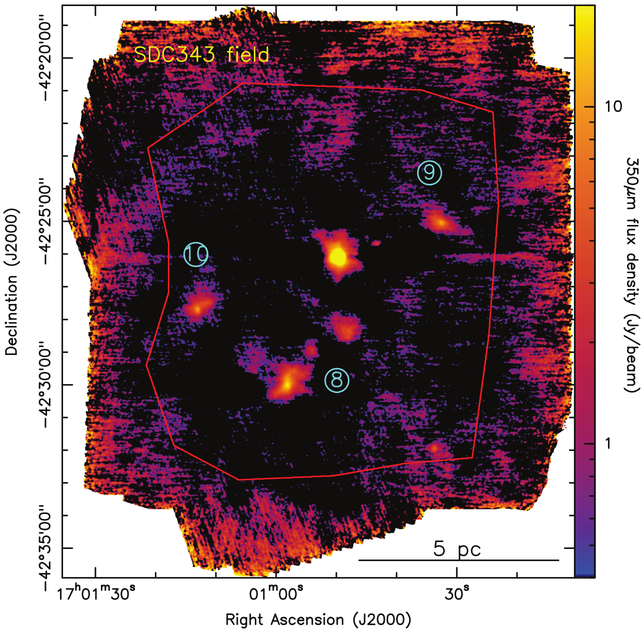

Figure A3. Same as Fig. 1 for the SDC343 field.

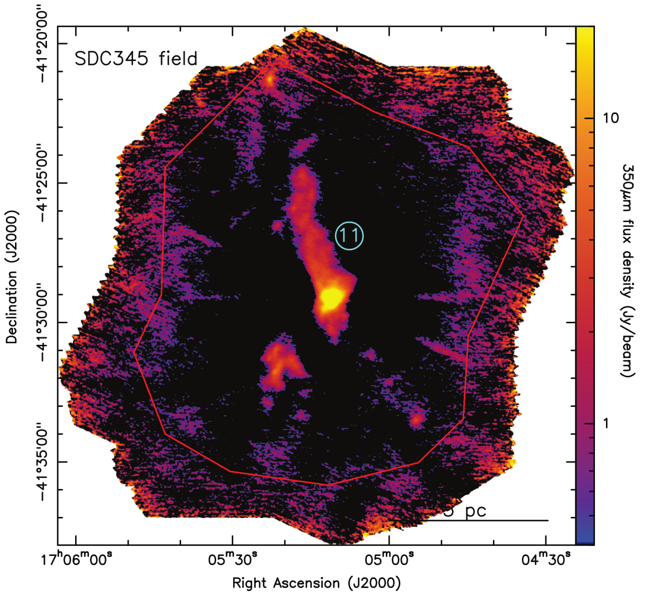

Figure A4. Same as Fig. 1 for the SDC345 field.

APPENDIX B: IMAGES OF ARTÉMIS SOURCES ASSOCIATIONS

In this Appendix, we present the ArTéMiS images with the locations of the *Herschel* 70-µm sources (Molinari et al. 2016), *Herschel* clumps (Elia et al. 2017), and ATLASGAL clumps (Csengeri et al. 2014) for the SDC326, SDC328, SDC340, SDC343, and SDC345 fields.

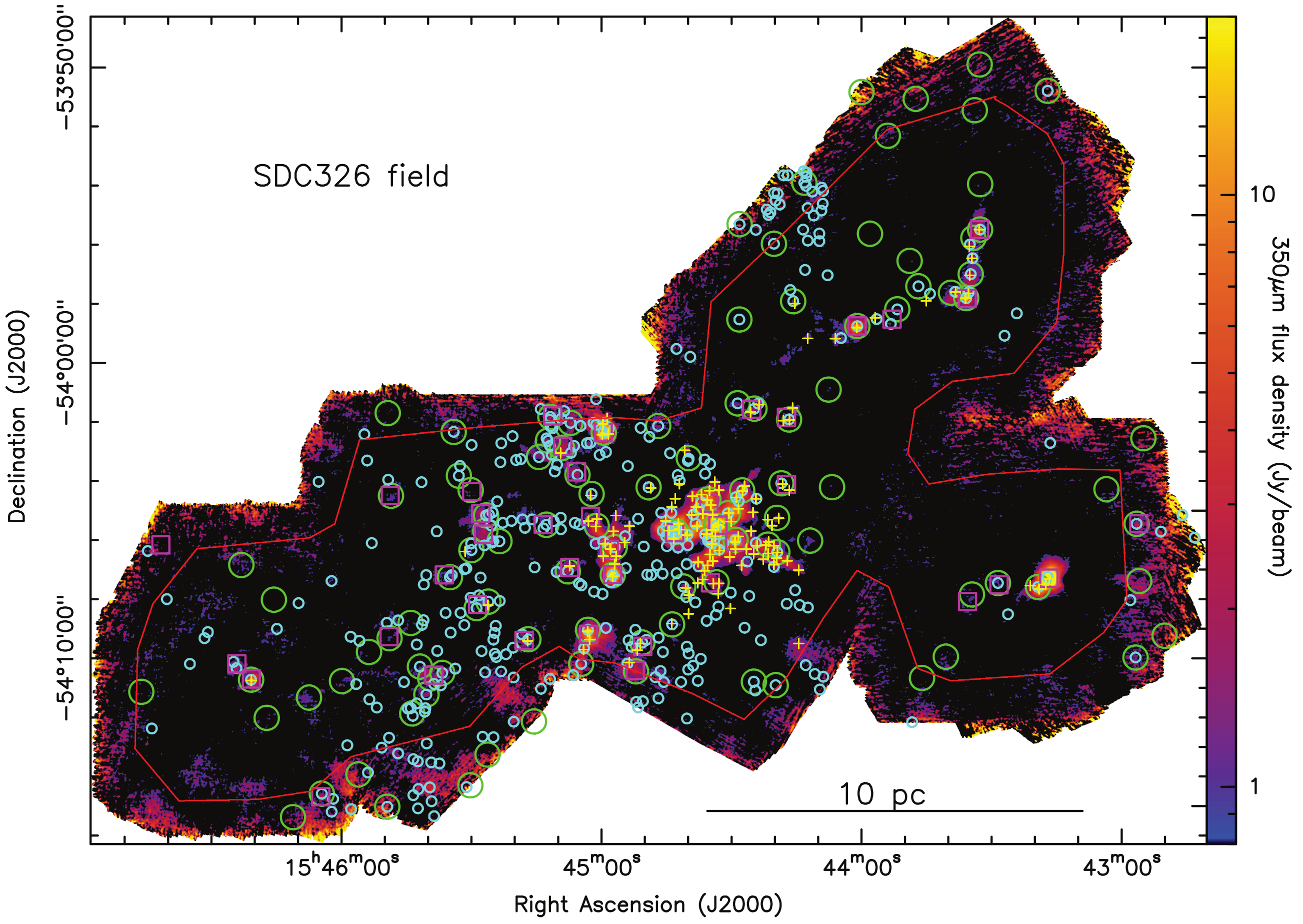

Figure B1. Background image is the same as in Fig. 1. The yellow crosses mark the central positions of the identified ArTéMiS sources. The cyan circles mark the central positions of the Hi-GAL 70-µm sources (Molinari et al. 2016). The green circles mark the central positions of the *Herschel* clumps (Elia et al. 2017). The purple squares mark the central positions of the ATLASGAL sources (Csengeri et al. 2014). The red solid line shows the area over which all source statistics presented in the paper have been calculated (i.e. excluding the noisy edges of the ArTéMis image).

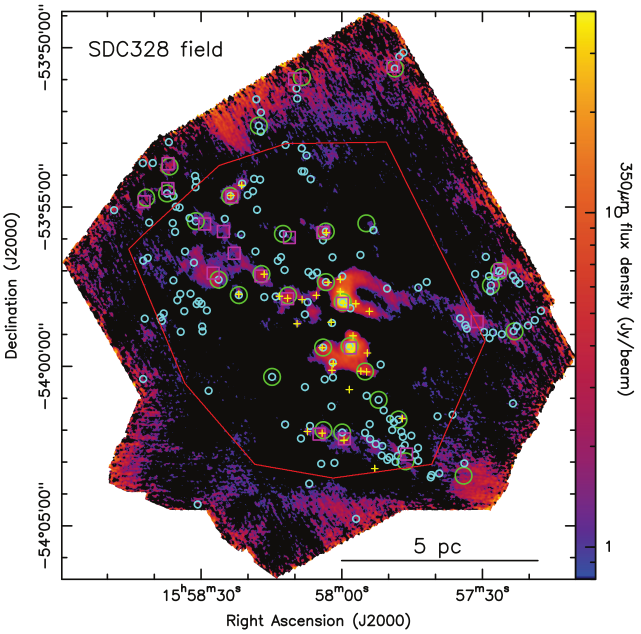

Figure B2. Same as Fig. B1 for the SDC328 field.

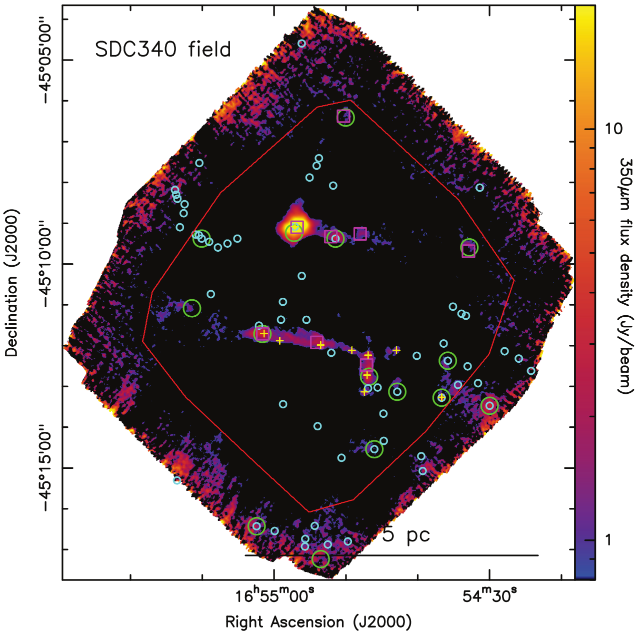

Figure B3. Same as Fig. B1 for the SDC340 field.

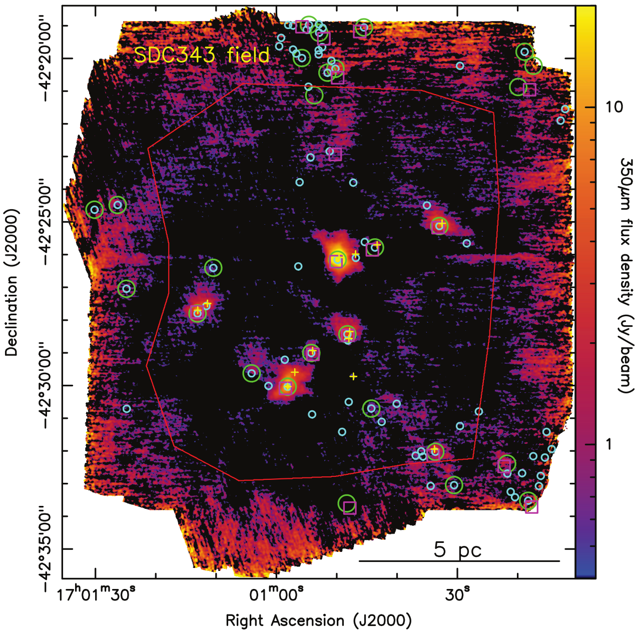

Figure B4. Same as Fig. B1 for the SDC343 field.

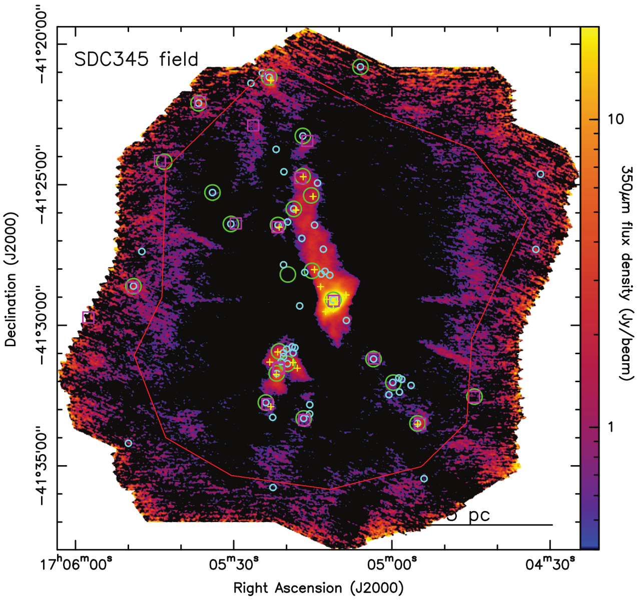

Figure B5. Same as Fig. B1 for the SDC345 field.